Ferroelectricity in the gapless quantum antiferromagnet NH_{4}CuCl_{3}

Jared S. Kinyon, Ronald Clark, Naresh S. Dalal, Eun S. Choi, and Haidong Zhou

Phys. Rev. B **92**, 144103 — Published 7 October 2015

DOI: 10.1103/PhysRevB.92.144103

Ferroelectricity in the Gapless Quantum Antiferromagnet NH_4CuCl_3

Jared S. Kinyon,* Ronald Clark, and Naresh S. Dalal†
Department of Chemistry and Biochemistry,
Florida State University, Tallahassee, FL 32306-4390

Eun S. Choi
National High Magnetic Field Laboratory, Tallahassee, FL, 32310-3706

Haidong Zhou
Department of Physics and Astronomy, University of Tennessee, Knoxville, TN 37996-1200

Ammonium trichlorocuprate, NH_4CuCl_3, a member of the family of quantum antiferromagnets M_3CuCl_3 (M = K, Tl, NH_4^+), well known for its gapless magnetization with unusual plateaus, is shown here to exhibit ferroelectricity below 67 K based on anomalies of the specific heat and dielectric constant, along with the appearance of spontaneous polarization and electric-field reversible pyroelectric current, making it a rare example of Cu(II)-based ferroelectric. This suggests that the general M_3CuCl_3 family could be rendered multiferroic by alloying its alkali metals with NH_4^+ ions.

PACS numbers: 75.85.+t, 77.80.-e, 77.80.B-, 82.60.Fa

I. INTRODUCTION

Multiferroic materials, compounds that combine magnetic and electrical ordering in the same phase, have experienced a renaissance in the past decade. One driving factors for their development is the potential for new technologies[1,2], one example being a coupling between the magnetic and electrical storage of data. Unfortunately theres paucity of multiferroics because the material characteristics needed for magnetism and ferroelectricity, for example the oxidation states of metal ions, are generally mutually exclusive[3,4]. Many interesting multiferroics are based on the perovskite frameworks, e.g. $BiMnO_3$[5] and Pb-based perovskites[6,7]. But material cost and environmental concerns have led to the development of new synthetic strategies, such as metal-organic hybrids without the heavy metals[8,9]. They have the perovskite framework, usually with a 3d transition metal ion bound with organic linkers as the A site and a mobile hydrocarbon ion as the B site. Interestingly, they exhibit many magnetic and dielectric properties similar to the heavier, inorganic perovskites but lack the hardness of the inorganic perovskites and high value of the saturated electric polarization.

In an effort to search for new families of magnetic ferroelectrics we took another approach: investigate a family of compounds that are known to exhibit unusual magnetic behavior but whose dielectric properties remain relatively unexplored. Our search led to the family of the $S = 1/2$ quantum magnets of the alkalimetal trichlorocuprate family $MCuCl_3$, where M = metal (K,Tl) or an ammonium ion. The $MCuCl_3$ family is considered to be a model for understanding quantum spin dynamics and dimerization of $S = 1/2$ molecules since it has been found to exhibit poorly understood quantum behavior at low temperatures[10–14]. For example, NH_4CuCl_3, henceforth abbreviated ACC, is unusual because (1) Although it is an antiferromagnet below 1.3 K, its magnetization exhibits no gap and thus no threshold for the change in the magnetization as function of magnetic field[10] (2) Its magnetization curve exhibits steps at $M/4$ and $3M/4$ before saturating at $M = 1.09\mu_B/Cu^{2+}$, in agreement with a multiple sub-lattice model[14]. (3) Other members need a threshold field, and their magnetization exhibits no steps.

In addition to the unusual magnetic behavior, ACC is also known to exhibit a structural phase transition (SPT) at about 70 K, as seen via NMR[15,16], ultrasonic attenuation[17] and neutron scattering[18]. The latter method detected a change in lattice dimensions in addition to a space group transformation from ($P2_1$ or $P\bar{1}$) to ($P\bar{1}$ or P1). Other members do not exhibit an analogous space group change. It seemed clear that this space group ambiguity could be clarified by examining whether the compound is polar or nonpolar, i.e. by measuring electric polarization since $P\bar{1}$ is a nonpolar group. In addition, the possibility of finding the compound to be polar was high because some compounds containing the $NH_4{}^+$ ion exhibit SPTs that are develop spontaneous polarization and become ferroelectric below the SPT. We thus focused on ACC for dielectric and thermodynamic measurements. As summarized herein, we find through dielectric constant and specific heat measurements that ACC indeed becomes ferroelectric below 67 K, which resolves the space group ambiguity and clearly clearly favors P1 over $P\bar{1}$. Measurements of ACC alloyed with other alkali metals suggest that it is forerunner of a new family of ferroelectrics with unusual quantum spin behavior, while additionally serving as a rare example of a Cu(II)-based ferroelectric.

II. EXPERIMENTAL METHODS

A. Synthesis and Crystallography

ACC was synthesized by the moisture-free method introduced by Willet et al[19]. Specifically, equimolar amounts of NH_4Cl and $CuCl_2$ were slowly dissolved in absolute ethanol in a dry nitrogen atmosphere, followed by slow evaporation at 60°C over several days, resulting in well-formed dark-red monoclinic needles several mm^3 dimensions that were found to be untwinned upon careful examination with a polarizing microscope. The known structure and bonding was authenticated through X-ray crystallography down to 100 K, in addition to face indexing for angular variation studies[19]. Similarly, a partially deuterated compound was grown under the same conditions; in this case, an equimolar solution of ND_4Cl and $CuCl_2$ in CH_3CH_2OD was allowed to slowly evaporate under constant nitrogen flow in an atmosbag from Sigma Aldrich. The extent of deuteration was ascertained by mass spectroscopy.

For X-ray studies, samples were cut from large, well formed single crystals and mounted onto a nylon loop with the use of heavy oil, typically Paratone-N. They were then mounted on a Bruker SMART APEX II diffractometer equipped with a graphite monochromator and Mo $K\alpha(\lambda = 0.71073\mathring{A})$ radiation source lying 6 cm from the CCD detector. The crystals were usually cooled to low temperatures for data collection in order to protect them from moisture. Integration was carried out with SAINT[20] and absorption corrections by SADABS[20], both of which are part of the Bruker suite of programs. XPREP[21] could then be used to obtain an indication of the space group, with the structure usually being solved solved through direct methods and refined by SHELXTL[22]. All but the hydrogen atoms were refined anisotropically, while the hydrogen atoms could be found during the least squares refinement. In practice, they are constrained as a riding model, but every effort was made to model any observed disorder.

Samples of $(NH_4)_xK_{1-x}CuCl_3$ were grown in a manner very similar to pure ACC, with of acetonitrile being used as a solvent instead of ethanol. First, a measured amount of KCl was slowly dissolved into a warm acetonitrile solution with constant stirring until saturation was achieved. The same step was separately carried out with NH_4Cl and anhydrous $CuCl_2$ in its own respective CH_3CN solutions. Given both the mass and volume of solvent added, the concentration of each solution could be found. From this, the appropriate amount of each solution could be added together such that the molar ratio of each component was 1:x:1-x = $CuCl_2$:NH_4Cl:KCl. The final mixture could then be heated slowly to 333 K in a warm heating bath and allowed to slowly evaporate. The

crystals took on the same appearance as the original compounds, i.e. long reddish needles.

It seems useful to briefly outline our procedure for solving the crystal structures of the mixed lattices. Consider, a mixture of potassium and ammonium ions would not possess an average electron count of 19 or 7, but instead have some intermediate value. The easiest route for solving the structure was often to assign the cation position with a fake atom that has a Z value somewhere in-between those used in the preliminary efforts. Then, the ratio could be obtained by entering the two correct elements into the instruction file and assigning them the same position, with subsequent commands ensuring both this and the equivalence of the atomic displacement parameters. Finally, the optimal ratio could be found through use of the PART command and subsequent cycles of least squares refinement. Figure 1 depicts a schematic of the unit cell at room temperature showing the dimerization, Cu−Cu contacts and possible hydrogen bonding for ACC.

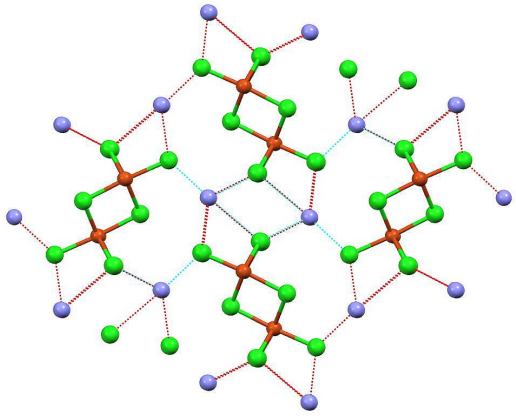

FIG. 1. Unit cell of NH_4CuCl_3. Cu^{2+} (Red), Cl^- (green), and turquoise (NH_4^+) ions viewed along the *a*-axis . Dotted lines show likely N−H···Cl hydrogen bonding.

B. Dielectric Constant and Polarization

Dielectric measurements were made on pellet as well as single crystal samples using an Andeen Hagerling capacitance bridge and the Quantum Design MPMS for temperature and magnetic field control. The bridge is capable of measuring both the real and imaginary signal using frequencies from 700 to 10,000 Hz, while the MPMS is capable of reaching a minimum temperature of 1.8 K and a maximum field of 7 T. The samples were given a parallel capacitor geometry, with silver paint being used for electrical contacts on two flat, parallel surfaces of the sample. The capacitance could then be measured and converted to the dielectric constant from the electrode area A and thickness d.

For spontaneous polarization (P_s) measurements, the capacitance bridge was replaced with Keithley 6517A electrometer. The samples were first slowly cooled using a polling field ranging from -10 to 10 kv/cm past the phase transition temperature in order to align electric dipoles within the sample. The applied field was then removed and the sample short circuited in order to remove any surface charges. Upon warming the sample, the change in pyroelectric current with respect to time, $I(t)$, could be used to obtain the polarization with knowledge of the heating rate $\frac{dT}{dt}$ using eq. (1). Measurements were repeated in magnetic fields of up to 7 T, but no significant effect was found.

$$P = \frac{1}{A\left(\frac{dT}{dt}\right)} \int_{T_i}^{T_f} I(t)\,\mathrm{d}T \qquad (1)$$

C. Heat Capacity

A Model 6000 Quantum Design Physical Property Measurement System (PPMS) was used for measuring the specific heat (C_p) at a constant pressure with the thermal relaxation. The measurement was carried out in a puck, which consists of a centered alumina platform

connected by a small set of thin wires. The wires structurally support the platform, in addition to providing a thermal connection with the puck and current conduction for the platform heater. The sample maintains thermal contact with the platform through a thin layer of Apiezon N-grease at high vacuum, while the temperature is measured with a Cernox thermometer.

During a measurement, the platform heater provides a pulse of heat, $P_H(t)$, momentarily raising the temperature of the thermally coupled sample platform above that of the puck frame, T_b. The difference between these temperatures, usually only 2% of the initial T_b, is then allowed to relax to its original state. If the sample is well coupled to the platform, then a simple exponential fitting model is used to extract C_p, which is found from eq. (2). Here, τ is the relaxation time, which is related to C_p and wire conductance as $C_p = \frac{\tau}{K_w}$. C_p can be found by subtracting the contribution from the grease and platform, also known as the addenda, from C_{total}[23].

$$T(t) = T_b + \Delta T \left(1 - e^{-t/\tau}\right) \tag{2}$$

For a more detailed view of phase transition, we resorted to a well known scanning method introduced by Bachmann[24,25]. This is based on the idea that the temperature response curve can provide information on the temperature dependence of $C_{\text{sample}}(T)$ within the range of the temperature rise, $T + \Delta T$. Thus, instead of obtaining only one heat capacity value with a single heat pulse, it is possible to obtain a dense number of specific heat values, limited only by the number of temperature readings. This is advantageous since it solves the problem of peak smearing and allows one to observe important features that may otherwise be missed in a sharp transition. The central equation for this analysis is found by rearranging the one-tau model and treating C_{total} is a function of temperature, the result of which is given in eq. (3). Here, $\mathrm{d}T/\mathrm{d}t$ is the derivative of the relaxation curve as a function of temperature, which is a reason that this technique is often called the slope method.

$$C_{\text{total}}(t) = \frac{P(t) - K_w\,(T - T_{\text{bath}})}{\mathrm{d}T/\mathrm{d}t} \tag{3}$$

III. EXPERIMENTAL RESULTS

A. Dielectric Constant

Figure 2 presents the pertinent dielectric data obtained using the standard parallel-plate method and silver paint for contacts, as has previously been described[8,26,27]. Measurements were made using frequencies from 700-10,000 Hz, with the presented data being taken at 2 kHz. These results were typical of the other frequencies, i.e. the underlying transition was devoid of any frequency dependence. Figure 2(b) shows the temperature dependence of ϵ', the real part of the dielectric constant over 1.8-120 K for a pellet sample of ACC, more specifically a thin disk with 3/16" outer diameter and thickness of about 0.2 mm. A clear λ-shaped peak is discernible at 67 ± 0.5 K, meaning that the earlier reported[15–18] SPT at this temperature involves a dielectric anomaly. The inset in fig. 2(b) shows a CurieWeiss plot $\frac{1}{\epsilon'} = \frac{(T-T_0)}{C}$, in the vicinity of the dielectric transition. For ferroelectric materials this relation should hold above the phase transition. For our pellet sample, $C = 4.47\times10^3$ and $T_0 = 7.1\times10^2$ K. A value of $C \approx 10^3$ is quite common for order-disorder ferroelectrics, as opposed to a displacive one in which $C \approx 10^5$ [28]. If one extends this analysis to below the phase transition, the lines intersect at 66.5 K, more formally be defined as T_c. In addition, $|C_{\text{low}}| = 2.90 \times 10^3$, making the ratio of the Curie constants in the high and low temperature phase, $\frac{C_{\text{low}}}{C_{\text{high}}}$, approximately two. This is a feature often present in second-order ferroelectric transitions such as that for $LiTIO_3$, which is triggered by the instability of a soft optic mode[28].

In order to find the polar axis, the dielectric constant was measured along crystallographic

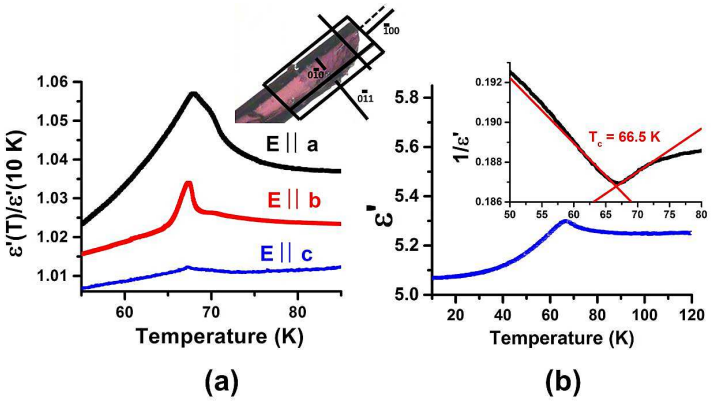

FIG. 2. (a) Temperature dependence of ϵ' of NH_4CuCl_3 along different crystallographic axes. Plots are normalized from their values at 10 K for clarity. Inset shows a face index of ACC (b) Temperature dependence of ϵ' at 2 kHz for a pellet sample. Inset is the Curie-Weiss plot.

directions a, b and c, identified from the aforementioned crystallographic studies. Figure 2(a) shows the normalized data, $\frac{\epsilon'(T)}{\epsilon'(10K)}$, along the three unit-cell directions, clearly providing evidence of anisotropy. Normalization was necessary because the parallel capacitor approximation does not hold well for the single crystal samples . The largest response is seen to be along the a-axis, which is also the longest crystal dimension. These directions are marked on the shown crystal. There is a small response along the b-axis, but none along the c-axis. No effort was made to detect the direction of the maximum dielectric response, but the ab plane must contain the polar axis, which essentially points along the a direction.

Another interesting feature of the curve can be seen upon closer inspection of the dielectric peak along the polar a-axis. On the high temperature side is a small shoulder, which suggests the presence of consecutive phase transitions. This peak was quite difficult to fit, so the derivative $d\epsilon/\mathrm{d}\,T$ was employed in order to find the maxima points. Again, it was found that the position of the phase transition points occurred at 69 and 67 K. This is quite interesting, as both acoustic[17], neutron diffraction[18] and ^{15}N-NMR[16] measurements detected the SPT to be at 70 K. It was only

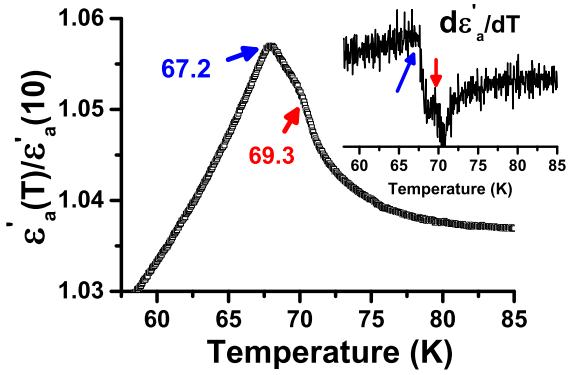

FIG. 3. Close view of the temperature dependence of the normalized (10 K) dielectric constant of ACC along the polar a-axis. Here, emphasis is placed on the presence of a shoulder, marked by the arrowhead, before the primary position of the transition around 68 K. For clarity, the inset shows the derivative of the primary curve in order to deduce the transition temperatures. The shoulder on the high temperature side suggests the presence of a double transition. The inset shows the derivative of the original points, and the maxima exposes two phase transitions at 69 and 67 K

the ^{14}N-NQR experiments[15] that suggested the presence of a second peak aside from that found at 70 K.

B. Polarization

A more definitive evidence for ferroelectricity can be seen in the polarization reversibility measurements under applied electric fields. The spontaneous polarization, P_s, was estimated from the pyroelectric current via eq. (1). Its values were integrated over a specified time to obtain the charge developed, Q, and divided by the electrode surface area as mentioned in eq. (1). Figure 4 shows a plot of P_s versus temperature at some typical applied electric fields, in both positive and negative directions along the a axis. It is readily seen that at least up to ± 10 kV/cm, the maximum available electric fields for our set-up, that P_s is completely reversible below 66.5 ± 0.5 K with a maximum value of ± 50 pC/cm^2. The temperature of the P_s onset coincides with the temperature of the dielectric peak maximum, confirming that T_0 (66.5 K) is indeed the ferroelectric transition. While the value of 50 pC/cm^2 is not as high as those for the inorganic perovskites, it is on the same order as other NH_4^+ based ferroelectrics[28]. Additionally, the definitive observation of P_s below T_0 implies that the space group of the ferroelectic phase must be polar, thus eliminating the ambiguity in neutron scattering that it might be either P1 or $P\bar{1}$: our results clearly support P1, which is also corroborated by ^{14}N-NMR data[15]. Despite incomplete knowledge of the low temperature phase, it seems reasonable to suppose that the electric dipole moment in the unit cell arises from N$-$H$\cdots$Cl bonds that distort the tetrahedral symmetry of the NH_4^+ ion and change its charge distribution, in addition to that of the $CuCl_3^-$ moiety. This would have the effect of removing the inversion center in the unit cell and inducing ferroelectricity in ACC.

The above-proposed hydrogen-bonding mechanism of the ferroelectric transition was supported by dielectric measurements on both (partially) deuterated samples and those mixed with the potassium ion. With a $\approx 50\%$ deuteration level, the transition shifted upwards from 67 to 71 K, indicating that order-disorder motion of the NH_4^+ ion must play a fundamental role in the mechanism of the ferroelectric transition. It would also explain why the K^+ and Tl^+ lattice variants would obliterate a potential ferroelectric transition.

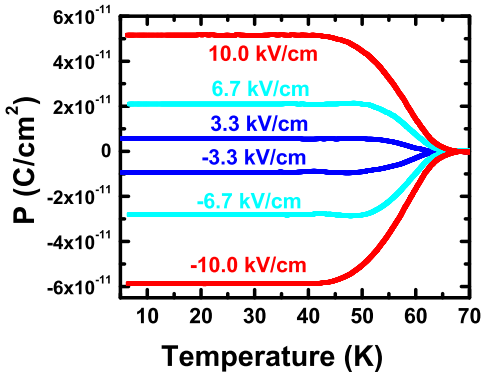

FIG. 4. Spontaneous polarization of ACC along the a-axis with a number of applied electric fields. Not all fields are included for clarity.

C. Specific Heat

Additional support for the order-disorder behavior of ACC was seen via specific heat measurements. Figure 5 shows two phase transitions over the range of 1.9-200 K. The first, $T_1 \approx 168$ K, is somewhat new but in agreement with earlier neutron diffraction data that detected the transition at 156 K[18], wherein it was interpreted as a transition involving the loss of a glide plane. These results corroborate the presence of that transition, though it gives no clear indication of the which phase to which it belongs. Below T_1 resides a second transition, $T_2 \approx 70$ K, which is very close to the position of the dielectric anomaly found at 67 K. Since previous evidence suggests that T_2 is structural in nature[17,18], while dielectric results that suggest ordering occurs due to the NH_4^+ ions, it seemed appropriate to find the mechanism responsible for the phase change and thus the ferroelectricity.

In order to verify our hypothesis that the

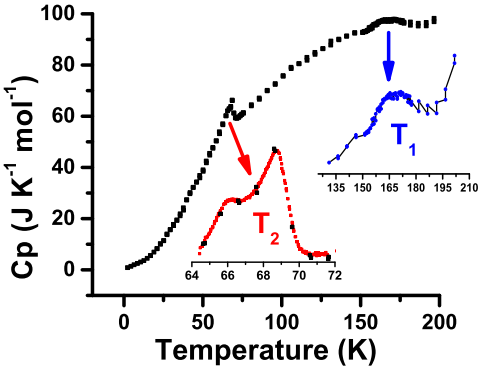

FIG. 5. Temperature dependence of the specific heat of ACC from 200 to 1.9 K. Transition Note the two transitions, T_1 and T_2, respectively at 168 and $\approx$ 68 K

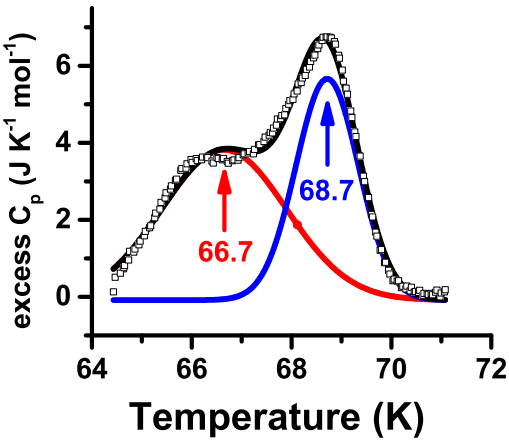

FIG. 6. Expanded view of the the dielectric phase transition, which reveals the presence of a double peak. Upon estimation of the baseline via Origin software, deconvolution was attempted with Gaussian curves. Though the fits are not ideal, they reasonably match with the ^{14}N-NMR splittings found at 69 and 67 K. Recall that the ferroelectric transition occurred at 67 K, which is likely when the ACC had arrived at the centrosymmetric phase

transition was of the order-disorder type, we calculated the excess transition entropy ΔS as the integral $\int \frac{C_p}{T}\,\mathrm{d}T$ over the peak and found it to be 0.30 J/(K mol), much less than the expected $R\ln 2 = 5.76$ J/(K mol) for a two-site order-disorder model. This is consistent with the fact that the C_p curve does not abruptly drop to zero below T_0, and that a significant part of the disorder still stays despite the setting-in of the ferroelectric ordering. Another consideration is that within the vicinity of the phase transition at $T < T_c$, the excess heat capacity $\Delta C = \frac{3}{2}R\left(\frac{T_c}{T}\right)^2$. When $T > T_c$, it follows that the order parameter for this model should go to zero, which implies $\Delta C = 0$. Accordingly, the maximum ΔC should be $\frac{3}{2}R$, or about 12.5 J/(K mol)[29]. When considering the baseline, the maximum heat capacity was around 7 J/(K mol), meaning that the excess specific heat also did not conform to the order-disorder model. All of this implies that the transition must be more complex than what is found in a simple order-disorder model. Because of the discrepancy from the dielectric data, more detailed studies on the structure of the low temperature phase are needed for a fuller explanation of the residual entropy.

Recall the second possible transition observed from the dielectric data. This was not readily observed with initial C_p measurements. But upon closer scrutiny, there was a double peak, as can be seen in both fig. 5 and fig. 6, indicating that a transition occurs in at least two steps. This was confirmed with measurements of multiple sample batches. Upon deconvolution by assuming two Gaussian curves, the peak temperatures are found to be 69 and 67 K, andd the respective area ratio approximately 3 to 4. This peak doubling has been reported elsewhere[15,30].

IV. MIXED CRYSTAL STUDIES

In order to extend the APC family, we grew mixed crystals of 90% APC and 10% $KCuCl_3$, i.e. $(NH_{4x})K_{1-x}CuCl_3$. Single crystal x-ray diffraction studies showed the mixed crystal to have the same crystal structure as APC, but the phase transition temperatures had significantly shifted. Figure 7 shows the tempera-

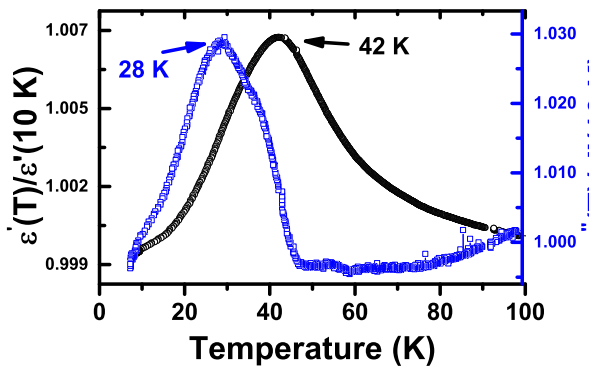

FIG. 7. Normalized temperature dependent dielectric constant, both real and imaginary, as a function of temperature.

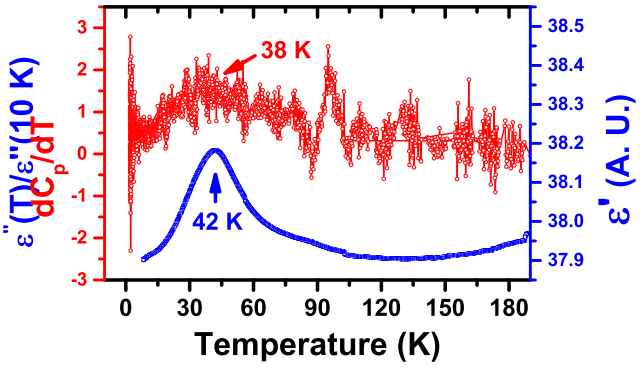

FIG. 8. A comparison of the dielectric constant and derivative of heat capacity with respect to temperature. Note that the respective peak positions at 42 and 38 K almost match, indicating th correlation of the heat capacity with the dielectric phase transition.

ture dependence of the dielectric measurements on $(NH_{4x})K_{1-x}CuCl_3$ Here, measurements were made on sample of ACC with 10% of the ammonium ions replaced by potassium. The first interesting result is that the transition temperature shifted by a significant margin, from 67 to 42 K. Second, the peak also extensively broadened, going from a sharp λ-type peak to one with a Full Width at Half Maximum (FWHM) of 25 K. Third, unlike ACC, a dispersion peak develops around 28 K with a slightly smaller FWHM of 20 K. The shoulder on the high temperature side lies at 38 K, which is very close to the original ϵ' peak, as would be expected. Fourth, the Curie constants are on the order of 10^5 K, significantly higher for this mix than for pure ACC. This value is much more consistent with displacive ferroelectrics like $BaTiO_3$. Fourth, there was no frequency dependence for either peak within the frequency range measured (5-20 kHz), indicating as for ACC that there were no soft modes within the measured frequency range and that the transition was thermodynamic in nature. Fifth, the transition is independent of the applied direction of the electric or magnetic field. Finally, the dielectric transition is extremely sensitive to the ammonium ion concentration. A very careful doping experiment would have to be carried out to produce a precise set of mixed compositions below 10% K^+concentration in order to see a clear trend between composition and T_c.

A direct plot of the specific heat vs temperature had no readily visible peak in the vicinity of the 42 K phase transition, as might be expected from the broadness of the dielectric peak. However, it was found that numerical differentiation of the specific heat with respect to temperature, that is, dC_p/dT, produced a broad hump. This may be interpreted as evidence for a phase change, which supports the dielectric results.

V. SUMMARY AND CONCLUSIONS

Measurements of specific heat, dielectric polarization and pyroelectric response of the magnetically well studied ACC shows that it undergoes a paraelectric-ferroelectric transition at 67 K with relatively little thermal hysteresis, a characteristic which is very typical of second-order transitions. The detection of the ferroelectric transition shows that the space group of the material must lose its center of symmetry, thus resolving an earlier ambiguity in the assignment of the low temperature phase as P1

rather than $P\bar{1}$. Likewise, an important finding is that the addition of alkali metals to APC results in isomorphic solid solutions. This is quite common in the field of hydrogen bonded ferroelectrics, where it has been shown that the NH_4^+ and the alkali metal ions can form continuous solid solutions if their size and charge are compatible[28]. For example, both K^+ and Tl^+ meet these criteria. In addition, we found that the ferroelectric T_c of APC shifted from 67 to 42 K even upon the addition of only 10% K. We thus surmise that ferroelectric character could be extended to the other members of the $MCuCl_3$ family. This is a rare example of Cu^{2+}-based ferroelectrics below 67 K and multiferroic near liquid-helium temperatures.

The authors would like to thank FSU for their partial support. In addition, the NHMFL is supported by NSF, DOE and the State of Florida via Cooperative Agreement DMR-0654118 and in part by NSF-DMR 1309146 (ESC).

---

* jkinyon@chem.fsu.edu
† dalal@chem.fsu.edu

[1] A. K. Cheetham and C. N. R. Rao, Science **318**, 58 (2007), http://www.sciencemag.org/content/318/5847/58.full.pdf.
[2] N. A. Spaldin, S. W. Cheong, and R. Ramesh, Physics Today **63**, 38 (2010).
[3] D. Bondurant, Ferroelectrics **112**, 273 (1990), http://dx.doi.org/10.1080/00150199008008233.
[4] H. Kohlstedt, Y. Mustafa, A. Gerber, A. Petraru, M. Fitsilis, R. Meyer, U. Böttger, and R. Waser, Microelectronic Engineering **80**, 296 (2005), 14th biennial Conference on Insulating Films on Semiconductors INFOS 2005.
[5] C. H. Ahn, K. M. Rabe, and J. M. Triscone, Science **303**, 488 (2004), http://www.sciencemag.org/content/303/5657/488.full.pdf.
[6] M. Bibes and A. Barthelemy, Nat Mater **7**, 425 (2008).
[7] K. Wang, J. M. Liu, and Z. Ren, Advances in Physics **58**, 321 (2009), http://dx.doi.org/10.1080/00018730902920554.
[8] P. Jain, V. Ramachandran, R. J. Clark, H. D. Zhou, B. H. Toby, N. S. Dalal, H. W. Kroto, and A. K. Cheetham, Journal of the American Chemical Society **131**, 13625 (2009).
[9] P. Jain, N. S. Dalal, B. H. Toby, H. W. Kroto, and A. K. Cheetham, Journal of the American Chemical Society **130**, 10450 (2008), pMID: 18636729, http://dx.doi.org/10.1021/ja801952e.
[10] H. Tanaka, W. Shiramura, T. Takatsu, B. Kurniawan, M. Takahashi, K. Kamishima, K. Takizawa, H. Mitamura, and T. Goto, Physica B: Condensed Matter **246-247**, 230 (1998).
[11] W. Shiramura, K.-i. Takatsu, H. Tanaka, K. Kamishima, M. Takahashi, H. Mitamura, and T. Goto, Journal of the Physical Society of Japan **66**, 1900 (1997), http://dx.doi.org/10.1143/JPSJ.66.1900.
[12] A. Oosawa, M. Ishii, and H. Tanaka, Journal of Physics: Condensed Matter **11**, 265 (1999).
[13] A. Oosawa, T. Takamasu, K. Tatani, H. Abe, N. Tsujii, O. Suzuki, H. Tanaka, G. Kido, and K. Kindo, Phys. Rev. B **66**, 104405 (2002).
[14] W. Shiramura, K. ichi Takatsu, B. Kurniawan, H. Tanaka, H. Uekusa, Y. Ohashi, K. Takizawa, H. Mitamura, and T. Goto, Journal of the Physical Society of Japan **67**, 1548 (1998).
[15] K. Kodama, M. Takigawa, and H. Tanaka, Progress of Theoretical Physics Supplement **159**, 228 (2005), http://ptps.oxfordjournals.org/content/159/228.full.pdf+html.
[16] Y. Shimaoka, T. Goto, K. Kodama, M. Takigawa, and H. Tanaka, Physica B: Condensed Matter **329–333**, 894 (2003), proceedings of the 23rd International Conference on Low Temperature Physics.
[17] S. Schmidt, S. Zherlitsyn, B. Wolf, H. Schwenk, B. Lthi, and H. Tanaka, EPL (Europhysics Letters) **54**, 554 (2001).
[18] C. Rüegg, M. Oettli, J. Schefer, O. Zaharko, A. Furrer, H. Tanaka, K. W. Krämer, H. U. Güdel, P. Vorderwisch, K. Habicht, T. Polinski, and M. Meissner, Phys. Rev. Lett. **93**, 037207 (2004).
[19] R. D. Willett, J. Claudius Dwiggins, R. F. Kruh, and R. E. Rundle, The Journal of Chemical Physics **38**, 2429 (1963).

[20] S. SADABS, Madison, Wisconsin, USA (1997).
[21] G. Sheldrick, Siemens Analytical X-ray Instruments (1991).
[22] G. M. Sheldrick, Acta Crystallographica Section A **64**, 112 (2008).
[23] Q. Design, *Physical Property Measurement System: Heat Capcacity Option User's Manual, Part Number 1085-150, M2*, San Diego, CA USA, 22nd ed. (2013).
[24] R. Bachmann, F. J. DiSalvo, T. H. Geballe, R. L. Greene, R. E. Howard, C. N. King, H. C. Kirsch, K. N. Lee, R. E. Schwall, H. Thomas, and R. B. Zubeck, Review of Scientific Instruments **43**, 205 (1972).
[25] K. N. Lee, R. Bachmann, T. H. Geballe, and J. P. Maita, Phys. Rev. B **2**, 4580 (1970).
[26] R. Samantaray, R. J. Clark, E. S. Choi, H. Zhou, and N. S. Dalal, Journal of the American Chemical Society **133**, 3792 (2011), pMID: 21355591, http://dx.doi.org/10.1021/ja1117683.
[27] R. Samantaray, R. J. Clark, E. S. Choi, and N. S. Dalal, Journal of the American Chemical Society **134**, 15953 (2012), pMID: 22978349, http://dx.doi.org/10.1021/ja3065705.
[28] M. E. Lines and A. M. Glass, *Principles and Applications of Ferroelectrics and Related Materials* (Oxford University Press, 2001).
[29] A. Tari, *The specific heat of matter at low temperatures* (Imperial College Press Distributed by World Scientific Pub. Co, London River Edge, NJ, 2003).
[30] C. Rüegg, Ph.D. thesis, ETH Zurich (2005).